The International Journal of Advanced Manufacturing Technology (2022) 119:3141–3155
https://doi.org/10.1007/s00170-021-08422-3

ORIGINAL ARTICLE

Liquid nitrogen in the industrial practice of hot aluminium extrusion: experimental and numerical investigation

Riccardo Pelaccia[1] · Barbara Reggiani[1] · Marco Negozio[2] · Lorenzo Donati[2]

Received: 1 September 2021 / Accepted: 21 November 2021 / Published online: 6 January 2022

Abstract

Nowadays, the liquid nitrogen cooling in aluminium extrusion is a widely adopted industrial practice to increase the process productivity as well as to improve the extruded profile surface quality by reducing the profile exit temperatures. The cooling channels are commonly designed on the basis of die maker experience only, usually obtaining modest performances in terms of cooling efficiency. Trial-and-error approach is time and cost consuming, thus providing a relevant industrial interest in the development of reliable numerical simulations able to foresee and optimize the nitrogen cooling effect during the die design stage. In this work, an extensive experimental campaign was performed during the extrusion process of an AA6060 industrial hollow profile, in different conditions of nitrogen flow rate and ram speed. The monitored data (die and profile temperatures and extrusion load) were compared with the outputs of a fast and efficient numerical model proposed by the authors, and developed in the COMSOL Multiphysics code, able to compute not only the effect of nitrogen liquid flow but also the gaseous condition. The results of the simulations showed a good agreement with experimental data, and evidenced how far the experimental cooling channel design from an optimized condition was.

Keywords Nitrogen cooling · Extrusion · Monitoring process · FEM · COMSOL

1 Introduction

The hot aluminium extrusion is a well-consolidated industrial manufacturing process able to produce profiles of complex geometry, such as multi-hollow shapes and thin sections, by imposing high deformation rates [1, 2]. The temperatures and the thermal gradients involved during the process affect its efficiency in terms of billet formability, profile quality as well as productivity and die lifetime [1–4]. Indeed, the control over the temperature is mandatory to optimize the extrusion process. If the billet pre-heating is required in order to suitably extrude the alloy, the deformation energy and the friction forces between the billet and the tools can lead to an excessive increase of temperatures both in the die and in the profile. This excessive exit profile temperature can cause several aesthetical defects or cracks on the profile surface, resulting in the scrap of the products or in the reduction of the service life of the tools [4–8]. The exit profile temperature strongly increases also with extrusion speed, thus generating relevant constraint in term of maximum achievable productivity [4].

Nowadays, the use of nitrogen cooling in aluminium extrusion dies is a well-known technology aimed at increasing the process speed, reducing die and tools temperature and improving the extruded profile surface quality [9, 10]. Several papers on gas and liquid nitrogen applications aimed at increased die performances were presented at the International Aluminium Extrusion Technology (ET) seminars [11–13]. Among the different tested solutions, liquid nitrogen was proved to be the most efficient one leading to double the extrusion speed [9, 13]. In a different study, Donati et al. [14] monitored the thermal gradient during the extrusion of a hollow profile in uncooled and cooled conditions with liquid nitrogen, obtaining a decrease of temperature up to 80 °C nearby the bearing zones.

In the current industrial practice, the cooling channel is realized in the backer element of the die set and positioned close enough to the bearings zones, where the extruded

✉ Riccardo Pelaccia
riccardo.pelaccia@unimore.it

[1] DISMI Department of Sciences and Methods for Engineering, University of Modena and Reggio Emilia, Via Amendola 2, 42122 Reggio Emilia, Italy

[2] DIN Department of Industrial Engineering, University of Bologna, Viale Risorgimento 2, 40136 Bologna, Italy

profile gets its final shape and where, consequently, the highest temperatures are reached (Fig. 1). Specifically, channels are milled on the backer face in contact with the die and a number of transferring holes shift the nitrogen to the profile surface (Fig. 1c). A greater cooling efficiency could be achieved by manufacturing the channels directly in the die, around the bearings; but this solution would require additive manufacturing technologies associated to greater costs, as discussed in the work of Reggiani and Todaro [15]. In both solutions, the cooling is localized nearby the profile exit, not involving the massive part of the deforming material and consequently minimally influencing the extrusion load.

The nitrogen in the liquid phase subtracts heat from the tooling set and then, in a gaseous phase, chills the profile surface and prevents the profile oxidation [16, 17]. However, nitrogen easily changes its state in gas when the temperature is higher than −196 °C at 1 bar [18]. This change means that different nitrogen phases may co-exist in the cooling channel. At the beginning of the extrusion process, the whole cooling channel (Fig. 1c) is free from nitrogen, then, after the nitrogen valve opening, the channel is gradually filled by liquid nitrogen that immediately evolves in a gaseous state as a consequence of the hot backer. After some seconds, the channel nearby the inlet is gradually filled by liquid nitrogen while gaseous nitrogen is present in the remaining sections of the channel. Only after some minutes that the cooling channel can be entirely filled by liquid nitrogen, while gaseous nitrogen can be found only after transferring holes. An optimized channel design promotes a transition to full liquid state within few extrusion runs, while a bad design may require several runs (up to never achieving the complete transition). The difference in terms of cooling effectiveness between the liquid and the gas nitrogen is relevant since the liquid nitrogen heat capacity is about 1.8 times higher than the gaseous one. In addition, it has to be reminded that, during phase change from liquid to gas, nitrogen expands 177 times in volume [18], leading to a significant pressure loss throughout the channel and consequently to a reduction of the nitrogen flow rate under constant inlet pressure. It comes clear that a bad channel design may promote an excessive formation of gaseous nitrogen that obstructs the channel, drastically reducing the flow rate and consequently the cooling efficiency.

Despite the significant interest in the use of liquid nitrogen as a coolant in the extrusion process, a systematic methodology for the design of the cooling channel has not been proposed in literature yet. Indeed, in the industrial practice, the cooling channels are manufactured according to the designer's experience that replicate the shape of the profile as close as possible to the bearing zones, but without verified criteria to obtain an optimal cooling solution. On the other hand, the cooling performance depends on a large number of variables, such as the channel geometry (position, cross-sectional area, length, and path), inlet and outlet positions, flow rate, coolant properties and mould material thermal characteristics [19–21]. In this context, the use of numerical methods such as FEM (Finite Element Method) can be extremely useful for the analysis and selection of an optimal cooling solution in relation to the process parameters and the geometrical features of the profile. The FE process modelling is nowadays widely used in the extrusion field to predict the thermal gradient and the extrusion load during the process [22–26], as well as to predict the extrusion defects [27, 28] or to optimize the die strength and lifetime [29–32]. Nevertheless, the modelling of the cooling channels effect is not consistently available in the FEM codes yet. In literature, only a previous work of Reggiani and Donati [24] is available in which a 3D numerical model of the extrusion process integrated with a 1D model of single-phase liquid nitrogen cooling is presented and validated over a simplified case study.

In this context, the aim of the present work is to innovatively test the FE modelling of the cooling effect on a real complex industrial case study taking into account the different cooling conditions: channels fully filled by liquid nitrogen or by gaseous nitrogen. The innovative numerical part of the work then consisted in the development of a model able to compute not only the effect of nitrogen liquid flow but also the gaseous condition.

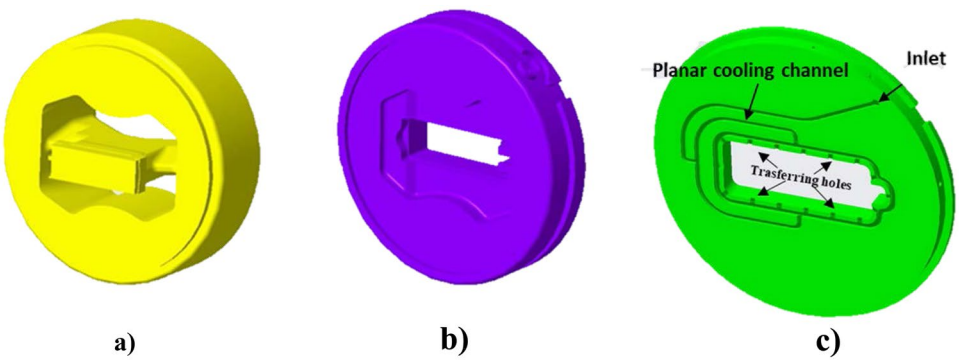

Fig. 1 Porthole die: **a** The mandrel; **b** the die; **c** the backer with the cooling channel

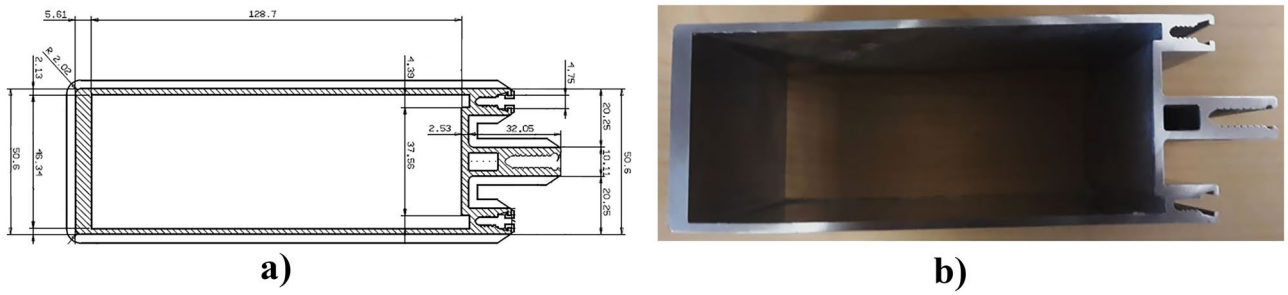

Fig. 2 The hollow profile selected for the experimental tests: **a** Profile drawing, **b** profile sample

The extrusion trails on the AA6060 hollow profile were performed in uncooled and cooled condition with different level of ram speed and nitrogen flow rate. The thermal data acquired by thermocouples in several locations of the die and of the backer were used to compare and to validate the numerical model. The global aim of the work is then to offer to the research community a more accurate model of the extrusion process cooled with nitrogen in order to better finalize the process optimization during the die design stage.

2 Experimental trials

2.1 Die design and liquid nitrogen cooling system

The hollow profile depicted in Fig. 2 was selected for the experimental tests. Three parts composed the tooling set: the mandrel, the die and the backer (Fig. 1). The mandrel, with two portholes, had an external diameter of 385 mm and the height of 112 mm in the extrusion direction. The die and the backer had the same external diameter of the mandrel, but the height of 72 mm and 23 mm respectively.

The nitrogen was provided in the die through the L-shaped circular inlet channel with a diameter of 8 mm, as reported in Fig. 3a, and it connected the nitrogen path to the planar channel, replicating the extrusion profile perimeter (Fig. 3b). The planar channel was milled at the backer face distant 33 mm from the bearings (Fig. 3a) with a square section (depth per width 3 × 5 mm and 4 × 6 mm as reported in Fig. 3b). Sixteen transferring holes (depth-per-width 2 × 5 mm) were also manufactured to lastly shift the nitrogen to the profile surface.

The liquid nitrogen, at a pressure of 7 bar, was stored in a large tank outside the industrial plant, with the nitrogen piped to the die through a pipeline with a length of about 100 m and a diameter of 15 mm. Before entering in the die, the nitrogen flows in the sub-cooler to obtain, at the entrance of the die, a nitrogen temperature in a liquid state below −196 °C. The maximum flow rate declared for this nitrogen plant is 80 kg/h when the valve is fully opened.

Eleven K-type thermocouples were used to monitor the thermal evolution during the extrusion process: six were located in the backer to follow the cooling channel path (P1 to P6 in Fig. 4b) while five were placed in the die (M3 to

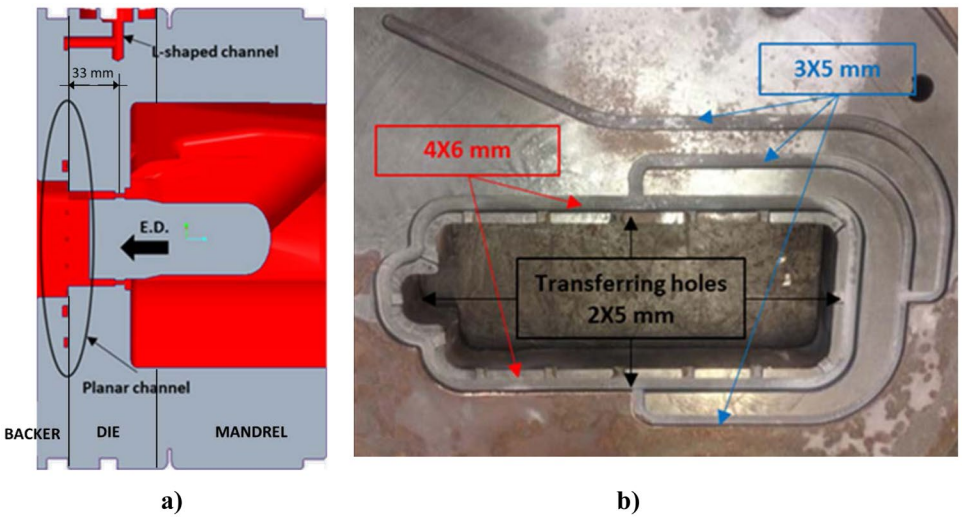

Fig. 3 The cooling channel design: **a** The L-shaped inlet channel; **b** the rectangular section design of the planar channel

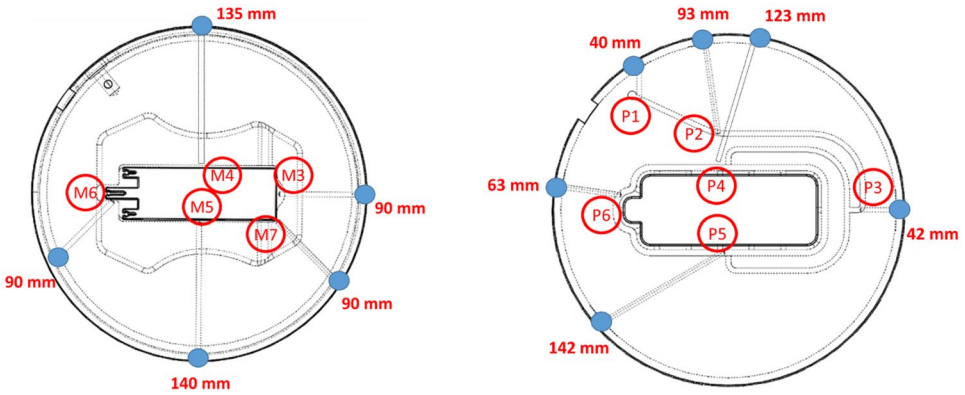

Fig. 4 Positions of the thermocouples: **a** Die, **b** Backer; numbers report the acquired depths of the thermocouple holes

M7 in Fig. 4a) to control the temperature around the bearing zones. During the installation of the thermocouples, the depth of the holes in the tooling set was verified and the quotes acquired and saved (Fig. 4).

In the die and the backer, an external rectangular-shaped groove was made to allow the thermocouples passage avoiding their breakage during the assembly in the ring (Fig. 5a, b). In addition, soft alloy pins were used for clamping the thermocouples further avoiding their misplacing.

2.2 Experimental campaign

The experimental campaign involved the extrusion of seventeen AA6060 billets in different conditions of extrusion speed and nitrogen flow rate (Fig. 6). The length and the diameter of the billets were 950 mm and 203 mm, respectively. A conical taper heating from 480 to 440 °C (front-back) was applied in the billet along its axis with the pre-heating die temperature set to 520 °C and the container temperature set to 400 °C.

Figure 7 reports the temperatures acquired by the thermocouples through an Agilent acquisition system connected to a laptop. The exit profile temperature was monitored at 1 m out of the press with a Williamson contactless pyrometer (black line in Fig. 7).

Trials started with the transfer of the die assembly from pre-heating oven (set at 520 °C) to the press and the thermocouples connection to the acquisition system (0–250 s). In Fig. 7, it is clearly visible that, during this time interval, the thermocouples placed in the backer (P1–P6) already registered lower values than thermocouples placed in the mandrel (M3–M6) as consequence of the greater heat exchange of the backer with the air and the die holder in the press. The thermocouple M7 got broken during die loading and it did not acquire valid data.

At around 400 s, the extrusion of the first billet started: temperatures in the die abruptly increased due to the hot aluminium flowing in the mandrel and in the die, while the temperature in the backer strongly decreased in relation to the greater heat transfer coefficient with the 'cold' press generated by extrusion load. Extrusion of billet 1 lasted up to 600 s due to the selected low ram speed (4 mm/s) and the stop for puller clamping of the profile.

During the dwell time for the billet change (600 to 900 s), the die cooled down, consequently heating up the backer that reached a thermal field close to the so called "steady-state condition of the uncooled process". From 900 s, three billets were extruded at the extrusion speed of 8 mm/s without any cooling to obtain, with billet 4, the steady-state condition for the uncooled process. The subsequent four billets were extruded at the same velocity, but with a nitrogen flow rate

Fig. 5 The installation of the thermocouples: **a** in the die and backer, **b** outside the external ring

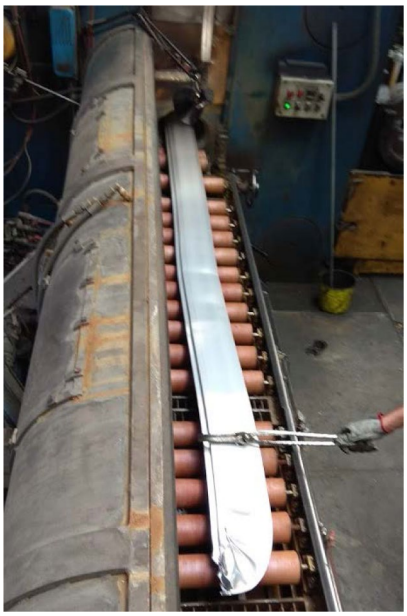

Fig. 6 The extrusion of the first billet

of the 40% and from billet 9 to billet 12 the liquid nitrogen flow rate was increased to the maximum. From billet 13 to the last billet, the extrusion speed was increased from 8 to 12 mm/s maintaining the 100% of nitrogen flow rate.

By analysing the thermal history of billet 4 that represented the steady-state condition of the uncooled process, an exit profile temperature of 556 °C was found, slightly lower than the peak temperature reached in the bearing zones. Indeed, thermocouple M3, positioned nearby the vertical part of the profile without wings (Fig. 4), recorded a peak temperature of 565 °C, the highest in the bearing zones. In addition, M6 (near the wings) and M5 (in the lower part of the profile) acquired a temperature only 5 °C lower than M3. The lowest temperature in the bearing zones has been recorded by M4, located symmetrically with respect to M5, with a maximum value of 525 °C. In the backer, the temperatures were much lower than in the die due to the several surfaces of the backer in contact with colder parts of the press. The lower temperature was registered in P1 (300 °C), which was located in the outer side of the backer at the entrance of the cooling channel. Thermocouples P3, P4, P5 and P6 were positioned as the corresponding thermocouples of the die, recording temperatures of 313 °C, 355 °C, 360 °C and 345 °C, respectively. The thermocouple P2, located nearby P1, provided a value of 311 °C.

Billet 8 was considered the steady-state condition for an extrusion speed of 8 mm/s and liquid nitrogen flow rate of 40%. With the selected channel design, the 40% of nitrogen flow rate was not enough to promote the liquid nitrogen flow through the cooling channel that was filled with gaseous nitrogen only. This was also experimentally confirmed by the absence of ice in the external surface of the nitrogen connecting pipe. Accordingly, Fig. 7 shows no significant changes in terms of thermal gradient in all the die thermocouples M3–M6, on the profile and in P1, while sensors in P2–P6 even showed a slight increase, as expected by a 'warm' gas nitrogen flow in the channel.

From billet 9, the valve of the nitrogen was opened to 100%, keeping the extrusion speed at 8 mm/s. Four billets

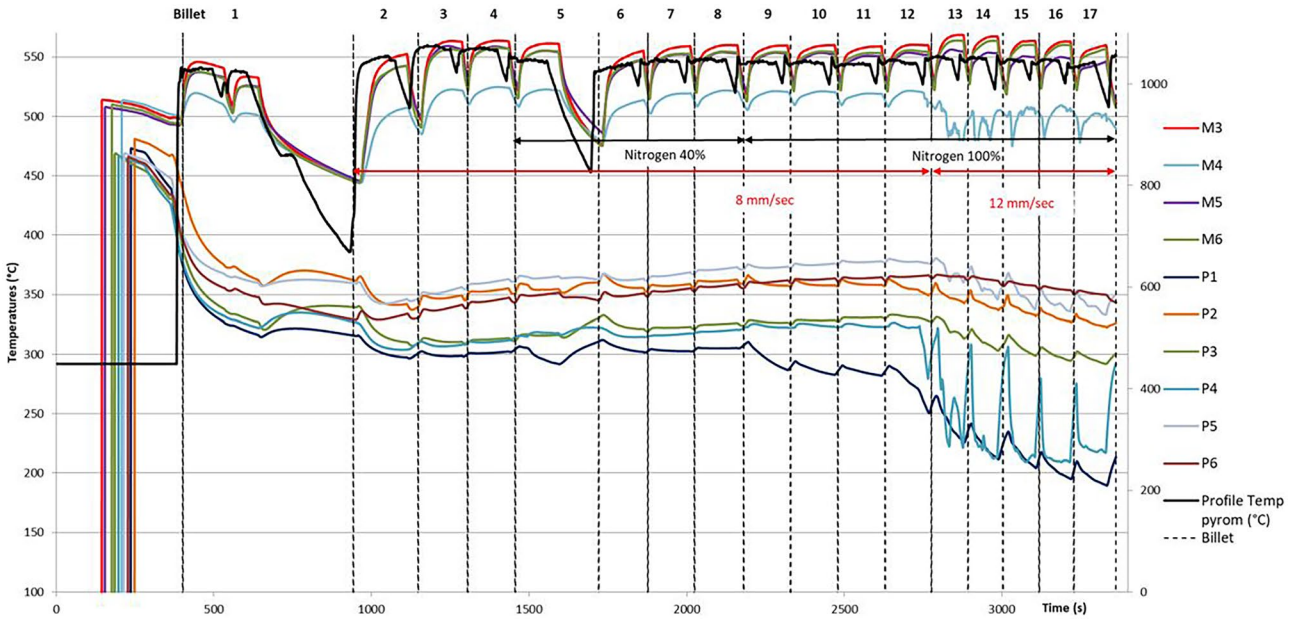

Fig. 7 Temperature history of the extrusion process: Thermocouples temperature and the exit profile temperature

(from 9 to 12) were extruded in this condition. The connecting pipe started to be partially covered by ice, as confirmed by thermocouple P1 that, as first, recorded a temperature of 250 °C against 300 °C of the uncooled condition. The effect of liquid nitrogen cooling reached P2 during billet 10 (at around 2.500 s) and reached P3 only during the extrusion of billet 12. The data suggest a very slow replacement of gaseous nitrogen by liquid nitrogen within the channel and the coexistence of gaseous and liquid nitrogen phases in the channel. A similar effect is visible for thermocouples P4 and P5. Again, the heat subtracted in the die was negligible. For further comparison with the numerical results discussed later in the paper, billet 12 was considered the steady-state condition for the extrusion speed of 8 mm/s and the 100% of nitrogen flow rate.

During the extrusion of billet 13, and subsequent billets, the extrusion speed was increased at 12 mm/s and the nitrogen valve was kept at maximum opening. In the backer, the mixture of gaseous and liquid nitrogen begun to show a visible cooling effect throughout the channel despite the greater generation of heat related to extrusion speed increase. At the beginning of the last extrusion, the connecting pipe was completely iced and the thermocouples P1 and P2 registered the highest drop of temperature with 196 °C and 219 °C against 300 °C and 311 °C of the uncooled condition, respectively. In the die, the cooling was less prominent but now visible and effective, obtaining a drop of 23 °C in M4 (from 525 to 502 °C) and of 13 °C in M5 (from 560 to 547 °C), while, in the profile, a decrease of around 10 °C (from 555 to 545 °C) was achieved. It has to be reminded that, together with temperature decrease, a 50% higher ram speed was used.

In terms of process loads, in the uncooled condition with a ram speed of 8 mm/s, a peak load of 23.3 MN (billet 4) was acquired while 24 MN was recorded in cooled conditions (billet 12). During the extrusion of the last five billets, the combination of increased ram speed and of the low cooling effect caused a limited raise of the extrusion load (below 10%), with a maximum registered value of 25.5 MN in billet 17.

In order to understand the behaviour of the nitrogen in the channel, it is possible to simplify the scheme as a tube with a pressure at the inlet, distributed pressure losses along the tube and outlet at atmosphere pressure (1 bar). If nitrogen enters as liquid and then changes its state in gaseous, an increase of volume of 177 times occurs thus preventing nitrogen flow. A good design of the cooling channel should lead to a condition with uniform temperatures all around the bearings but also to a short transient from gas to liquid.

Performed experimental trials highlighted the limits of the designed cooling system that was not as effective as expected. Temperatures in the backer and in the die were not uniform around the profile, with differences in the die from M3 to M4 up to 44 °C in the cooled condition (billet 12) and up to 58 °C in the cooled condition at higher extrusion speed (billet 17) with respect to the 35 °C of the uncooled condition (billet 4). Differences became much more relevant in the backer: in billet 17, a delta of temperature of 154 °C was found from P1 to P5 while, in billet 12, of 88 °C compared to 60 °C of the uncooled condition. The nitrogen flow rate of 40% was ineffective, probably due to the excessive pressure drops generated by the channel design. Too many extrusions were needed to generate the cooling effects in the backer, also with the nitrogen flow rate set to 100%. Moreover, the acquired data suggested that during the extrusion of the last billet, a mixture of gas and liquid nitrogen was still flowing into the cooling channel, thus indicating that the steady-state cooled condition still was not reached. The experimental data clearly showed that the cooling effect in the die was not effective both for the unoptimized channel design and for the great distance of the channel from the bearings (Fig. 3a).

In conclusion, the experimental campaign clearly showed the necessity of developing a reliable channel design criteria or numerical tools in order to gain optimal cooling

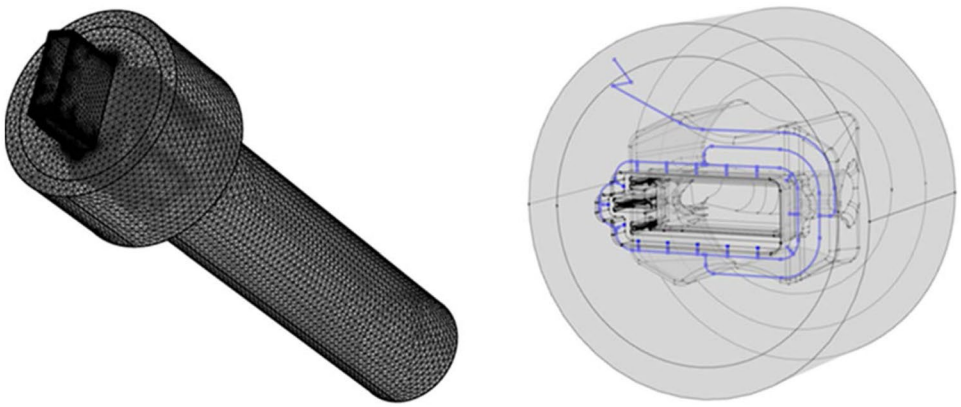

Fig. 8 The geometrical model for the simulation tests: **a** the billet and the die set for uncooled process, **b** the tooling set combined with the 1D cooling channel

Table 1 Flow stress parameters of Zener-Hollomon model for AA 6060

Flow stress parameters	AA6060
Q parameter of Zener-Hollomon model	161 kJ/mol
A parameter of Zener-Hollomon model	$7.6301*10^{10}$ 1/s
n parameter of Zener-Hollomon model	4.67
a parameter of Zener-Hollomon model	0.035 1/MPa

conditions. Indeed, the tested design seemed initially a good solution to the press technicians, but it actually turned out to be very ineffective.

3 Numerical modelling

3.1 Simulation setting of the industrial case study

The COMSOL Multiphysics software [31] allows integrating different modules for coupled modelling of thermal, structural and fluid dynamics problems. Therefore, it is possible to model the 3D extrusion process integrated with a 1D model of the channel for nitrogen cooling as showed by the authors in a previous work [24].

For aluminium extrusion simulation, the COMSOL code uses a pure Eulerian approach, thus requiring the input of the billet geometry in the already-deformed configuration (Fig. 8). Figure 8a shows the meshed 3D model of the tooling set and of the aluminium parts, while Fig. 8b presents the 1D channel integrated in the tooling set for the simulation with nitrogen cooling.

Concerning the aluminium flow stress, the Zener-Hollomon (inverse sine hyperbolic) model [33] was used (Eq. (1)), thus treating the hot aluminium as a non-Newtonian fluid with high viscosity related to temperature and strain rate [34]:

$$\tilde{\sigma}(T,\dot{\varepsilon}) = \frac{1}{\alpha} sinh^{-1}\left[\frac{1}{A}\dot{\varepsilon}\, exp\left(\frac{Q}{RT}\right)\right]^{\frac{1}{n}} \quad (1)$$

In Table 1, the parameters of the flow stress model for AA6060 are reported as found in literature [35].

The mandrel, the die, and the backer were combined into a single solid tool with the aim of simplifying the computation avoiding the contact analysis. The container and the ram were replaced by equivalent thermal and fluid-dynamic boundary conditions, thus further reducing the number of components and the required computational time. In the billet surface in contact with the ram, the velocity inlet condition was imposed equal to the ram speed and a temperature of 440 °C was set. In the billet surface in contact with the container, a temperature of 430 °C was imposed.

In the contact areas between the billet and the tooling set (ram and container included), a sticking friction condition was generally imposed, while in the bearing zones and in the exit profile surfaces the slip friction condition was used. Heat transfer coefficients of 11,000 W/m^2°K and 3000 W/m^2°K were set in aluminium-to-tool contacts and in tool-to-tool contacts, respectively [24, 36], while 30 W/m^2°K was set for the heat exchange with the external air. In the backer surfaces in contact with press, a heat flux with a constant temperature of 280 °C was imposed, experimentally suggested by the temperature of 300 °C registered by P1 in the steady-state uncooled condition. Accounting for the reviewer comment, the following sentence has been added in the text in Sect. 3.1 to detail how the mesh was generated: "The mesh was generated with the COMSOL environment. For the billet and the material inside the die, a mesh consisting in 1,200,053 tetrahedral

Table 2 Process parameters, boundary conditions and nitrogen properties for all simulations

Process parameters	Uncooled process	Gas nitrogen cooling	Liquid nitrogen cooling
Billet temperature	480 °C	480 °C	480 °C
Die temperature	510 °C	Initial value steady state uncooled simulation (end of Billet 4)	Initial value steady state uncooled simulation (end of Billet 4)
Container temperature	430 °C	430 °C	430 °C
Ram temperature	440 °C	440 °C	440 °C
Temperature of backer surfaces in contact with press	280 °C	280 °C	280 °C
Ram speed	8 mm/s	8 mm/s	12 mm/s
Inlet nitrogen temperature	-	−196 °C	−196 °C
Nitrogen flow rate	-	6.04 kg/h	80 kg/h
Surface roughness of the channel (e)	-	0.046 mm	0.046 mm
Nitrogen density (ρ)	-	4.56 kg/m^3	806.59 kg/m^3
Nitrogen heat capacity at constant pressure (C_p)	-	1.123 J/g*K	2.041 J/g*K
Nitrogen thermal conductivity (k)	-	0.00700 W/m*K	0.14605 W/m*K

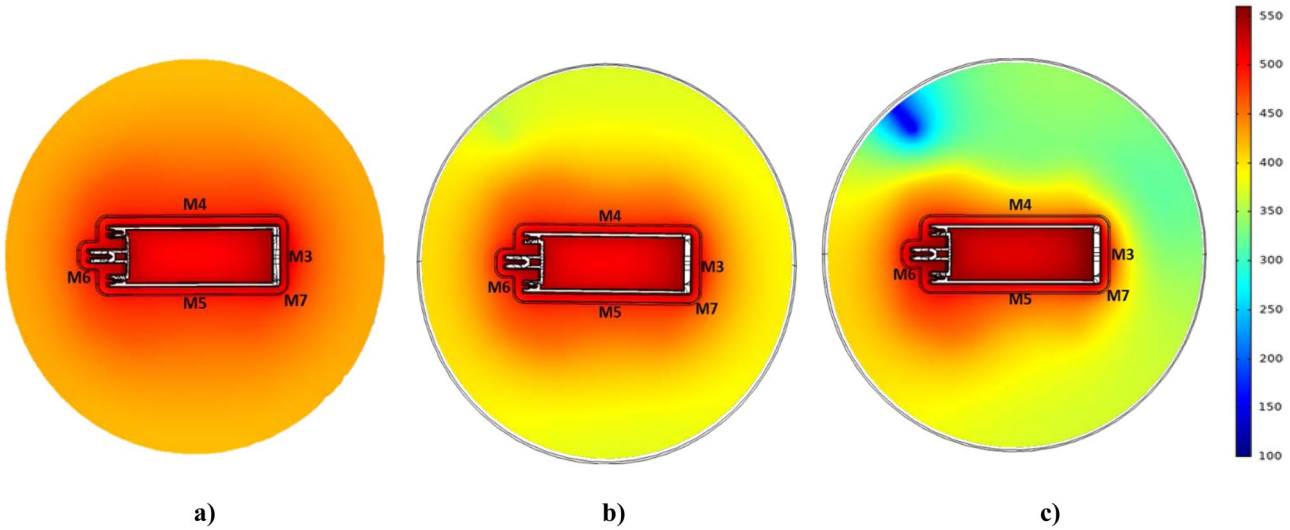

Fig. 9 Thermal map of the die after 600 s of simulation: **a** uncooled, **b** gas cooled process, **c** liquid cooled process

elements (size range 0.5–5 mm) was used. For the die, 953,700 tetrahedral elements (size range 1–10 mm) were used following the die geometry complexity. In the bearings and in the profile, instead, 202,000 hexahedral elements were imposed with a minimum of 5 layers of nodes along the profile thickness in order to guarantee an accurate computation of the temperature and velocity fields. For the cooling channel, a 1D mesh of 305 edge elements (size range 0.25–5 mm) was used.

Simulations were performed without any cooling for comparison with billet 4, with the model for gaseous nitrogen only as comparison with billet 12 and with the model for liquid nitrogen only as comparison with billet 17. Even if the phase change is not considered in this model, the analysis of the nitrogen thermal map allows locating the shift of phase of the nitrogen in the channel. Transient simulations were performed in order to represent the whole extrusion time experimentally processed.

The process parameters and the boundary conditions were set to replicate the experimental setting and they are reported in Table 2. Specifically, the uncooled simulation used, as initial values, the initial conditions of billet 1, while the cooled simulations both started with the steady-state condition obtained in the uncooled simulation (billet 4). In both simulations with nitrogen cooling, the same pressure gradient was imposed between the inlet and the outlets of the channels and equal to the amount needed to get 80 kg/h of liquid nitrogen flow rate. In Table 2, the physical properties of liquid and gas nitrogen at the boiling point at room pressure (−196 °C) [18] are also reported.

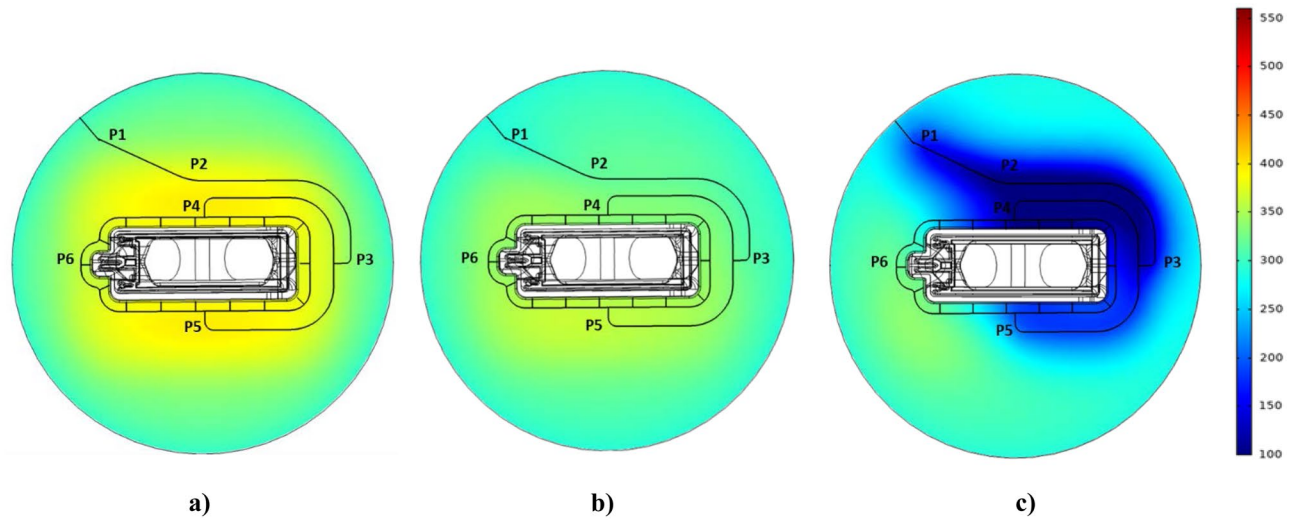

Fig. 10 Thermal map of the backer after 600 s of simulation: **a** uncooled, **b** gas cooled process, **c** liquid cooled process

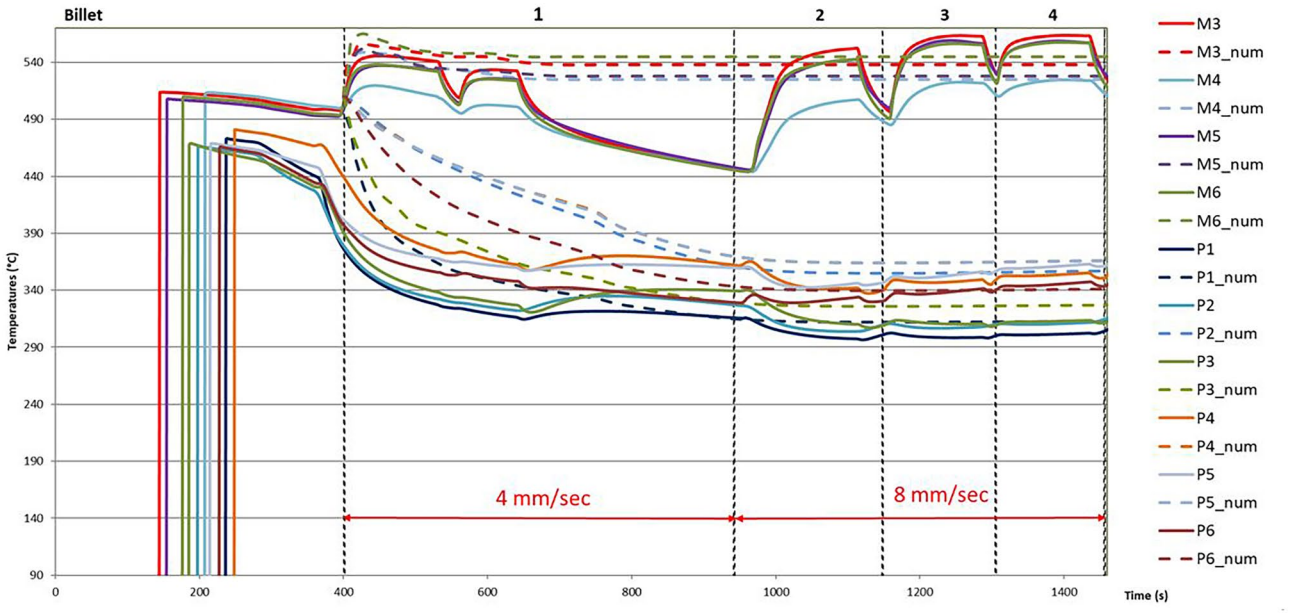

Fig. 11 Temperature history of the extrusion process: Experimental–numerical comparison without cooling

3.2 1D Nitrogen cooling modelling

The 1D cooling model approximates the pipe flow profile as mono-dimensional thus reducing the calculation to the mid-line path [20, 37]. In addition, it is possible to set the geometrical shape of the channel cross section for the evaluation of the fluid dynamic variables (Reynolds number, pressure drop, etc.). The model calculates the pressure and velocity of an incompressible or weakly compressible fluid (phase change is not considered), by solving the continuity and momentum equations (Eqs. (2) and (3)) reported in the following:

$$\frac{\partial A_c \rho}{\partial t} + \nabla \cdot \left(A_c \rho u\right) = 0 \tag{2}$$

$$\rho \frac{\delta u}{\delta t} = -\nabla p - f_D \frac{\rho}{2 d_h} u|u| \tag{3}$$

where ρ represents the density of the fluid, A_c the area of the channel section, u the velocity of the fluid along the channel, p the pressure of the fluid and d_h the hydraulic diameter of the channel.

The second term on the right-hand side of Eq. (3) accounts for pressure drop due to viscous shear. The pipe flow physics uses the Churchill friction model to compute the Darcy factor f_D, that it is valid for laminar flow, turbulent flow and the transition region. The Churchill friction model is given by Eq. (4), where A and B are the empirical coefficients that depend on the Reynolds number (R_e) and the surface roughness divided by diameter of the pipe, e/d_h.

$$f_D = 8 \cdot \left[\left(\frac{8}{Re}^{12} (A+B)^{-1.5} \right)^{\frac{1}{12}} \right] \tag{4}$$

$$A = \left[-2.457 \cdot ln((\frac{7}{Re}^{0.9} \left(\frac{e}{d_h} \right)) \right]^{16} \tag{5}$$

$$B = \left(\frac{37530}{Re} \right)^{16} \tag{6}$$

Concerning the prediction of the thermal field in the channel and of the thermal interaction between the nitrogen and the die [20, 37], the heat transfer equation is:

Table 3 Comparison between the experimental acquired temperatures in the backer and the predicted numerical results (Billet 4)

Billet 4	Thermocouples temperature [°C]						Cooling
	P1	P2	P3	P4	P5	P6	
Experimental	300	311	313	355	360	345	**NO**
Numerical	313	357	327	366	366	341	**NO**
Err%	+4.3%	+14.8%	+4.5%	+3.1%	+1.7%	−1.2%	

Table 4 Comparison between the experimental acquired temperatures in the die and the predicted numerical results (Billet 4)

Billet 4	Thermocouples temperature [°C]					Profile Exit T [°C]	Cooling
	M3	M4	M5	M6	M7		
Experimental	565	525	560	560		556	**NO**
Numerical	538	525	528	545	525	549	**NO**
Err%	−4.8%	0%	−5.7%	−1.3%		−1.3%	

$$\rho A_c C_p \frac{\partial T}{\partial t} + \rho A_c C_p u \cdot \nabla T = \nabla \cdot A_c k \nabla T + f_D \frac{\rho A_c}{2 d_h} u^3 + Q_{wall} \tag{7}$$

where C_p is the heat capacity at constant pressure, T the nitrogen cooling temperature and k the thermal conductivity. The second term on the right-hand side corresponds to the heat dissipated due to internal friction in the fluid. In addition, Q_{wall} is a source term that accounts for the heat exchange with the surrounding die:

$$Q_{wall} = hZ\left(T_2 - T\right) \tag{8}$$

$$\rho_2 C_{p2} \frac{\partial T_2}{\delta t} = \nabla \cdot k \nabla T_2 \tag{9}$$

In Eq. (8), Z is the perimeter of the pipe, T_2 is the temperature calculated in each point of the die, while h is the heat transfer coefficient. The latter depends on the physical properties of the fluid and on the nature of the flow, and it is calculated from the Nusselt number (N_u):

$$h = Nu \frac{k}{d_h} \tag{10}$$

As can be seen, h is not considered as constant along the cooling path, differently from what frequently imposed in the published literature.

The use of a 1D approach is preferred to 3D approaches, in order to avoid an excessive increase in the computational time without decreasing the reliability and the accuracy of the simulation.

The suggested approach then perfectly matches the requirement of supporting the die design phase in an industrial framework, even accounting for the possibility to rapidly modify the cooling channel design parameters, the position and the shape of the channels and also its cross-section for the achievement of the optimal solution.

4 Comparison between the numerical and the experimental results

The numerical predictions were compared with the experimental data in terms of temperatures and extrusion load. Figures 9 and 10 show the computed thermal map of the die and the backer in the thermocouple mid-plane for the three different cooling conditions.

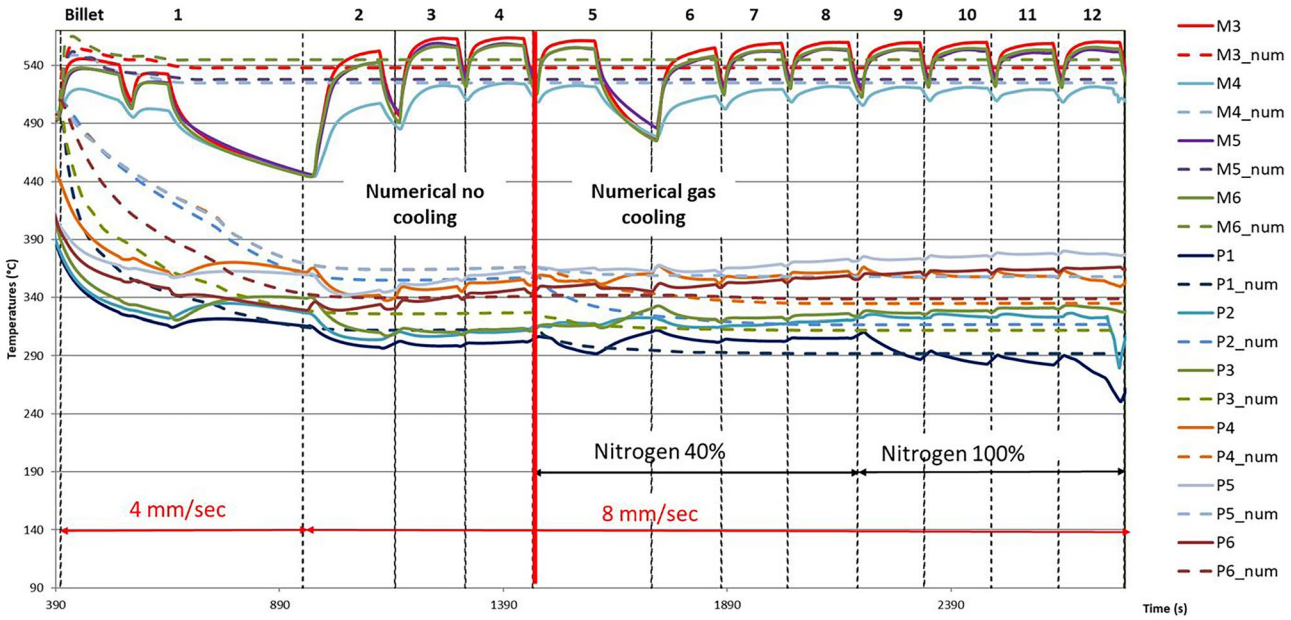

Fig. 12 Temperature history of the extrusion process: Experimental–numerical comparison in the gaseous cooled condition

Table 5 Comparison between the experimental acquired temperatures in the backer and the predicted numerical results (Billet 12)

Billet 12	Thermocouples temperature [°C]						Cooling
	P1	P2	P3	P4	P5	P6	
Experimental	272	325	329	351	360	347	**Gaseous**
Numerical	292	317	312	335	358	339	**Gaseous**
%Err	+7.4%	−2.5%	−5.2%	−4.6%	−0.6%	−2.3%	

In the simulation without cooling, the thermal map of Fig. 9a shows a range of temperatures around 560 °C nearby the bearings while the simulation with gas nitrogen cooling showed almost no temperature changes around the bearings (Fig. 9b) and a limited drop of temperatures towards the external surface of the die only. The simulated liquid nitrogen cooling was more effective, displaying the greater temperature drop around M4, M5 and M7, while a minor effect nearby M3 and M6.

In the backer, the thermal map of the gas cooled condition showed a small cooling effect, obtaining the maximum drop of temperatures of about 20 °C in the region around P1. The liquid nitrogen underlined a greater cooling effect, made clear by the deep blue region across the channel. However, the cooling turned out to be less effective around P5 and negligible nearby P6, thus clearly pointing out the limits of the channel design.

In Fig. 11, the experimental data of all the thermocouples were overlapped to the values computed by the simulation in the uncooled condition (billets 1 to 4). The Eulerian approach considers the billet as a continuous fluid that flows within the container and the die; thus, during the transient simulation, the model simulated the extrusion of a single virtual billet for 600 s. For this reason, numerical results in the die (M3-M6) showed an initial peak of temperatures generated by the billet in deformation then, after the transitory, the temperatures reached a steady-state condition. On the contrary, the experimental results showed a peak of temperatures and a cooling down during each billet change. Similar considerations can be drawn for backer locations (P1–P6) unless the initial thermal increase not detected in both experimental and numerical data.

The numerical results of the steady-state simulation in the backer showed a good matching with experimental data (error below 4.5%), with an overestimation only in P2 (357 °C num. against 311 °C exp.).

The numerical steady-state condition provided a drop of temperatures with respect to the initial transitory, related to the simulated billet cooling in the container. Indeed, the boundary condition in the billet replicated a heat flux with constant temperature equal to the container temperature (430 °C). This condition cooled excessively the "long virtual billet", while the preheated temperature of the real billets was higher. However, the maximum numerical underestimation of 32 °C registered in M5 (528 °C against 560 °C) did not affect the reliability of the predicted results.

In Tables 3 and 4, the experimental–numerical comparisons for the backer and the die in the steady-state uncooled condition are reported. The accuracy of the numerical predictions was assessed by the errors always below 6% in all thermocouples except for P2 (14.8%). In terms of extrusion load, a peak of 20.5 MN was predicted against 23.3 MN experimentally acquired, with an error of 12%.

In Fig. 12, the simulation of gaseous nitrogen cooling was compared to the experimental results. The numerical computation started from the steady-state uncooled thermal condition (end of billet 4) with gaseous model, 100% valve opening and 8 mm/s of ram speed. Results are plotted up to billet 12, when liquid nitrogen started providing a visible cooling effect. Indeed, the connecting pipe started to be covered by ice only from billet 12 while, during the previous extrusions, only gas nitrogen was flowing within the channel.

In the die, the numerical outcomes matched the experimental cooling inefficiency, further underlining the minor cooling effectiveness of gas nitrogen.

In the backer, during the extrusion of billets 5 to 11, a good accuracy of the numerical model was found for locations P1 to P3 while for locations P4 to P6, the simulation provided a slight underestimation of the temperatures. However, a better matching was achieved in locations P2 to P4 if data at the end of the billet 12 are analysed, with a numerical overestimation of the experimental temperature in P1 and

Table 6 Comparison between the experimental acquired temperatures in the backer and the predicted numerical results (Billet 12)

Billet 12	Thermocouples temperature [°C]					Profile Exit T [°C]	Cooling
	M3	M4	M5	M6	M7		
Experimental	560	516	552	554		545	**Gaseous**
Numerical	538	525	528	545	525	548	**Gaseous**
%Err	−3.9%	+1.7%	−4.3%	−1.6%		+0.6%	

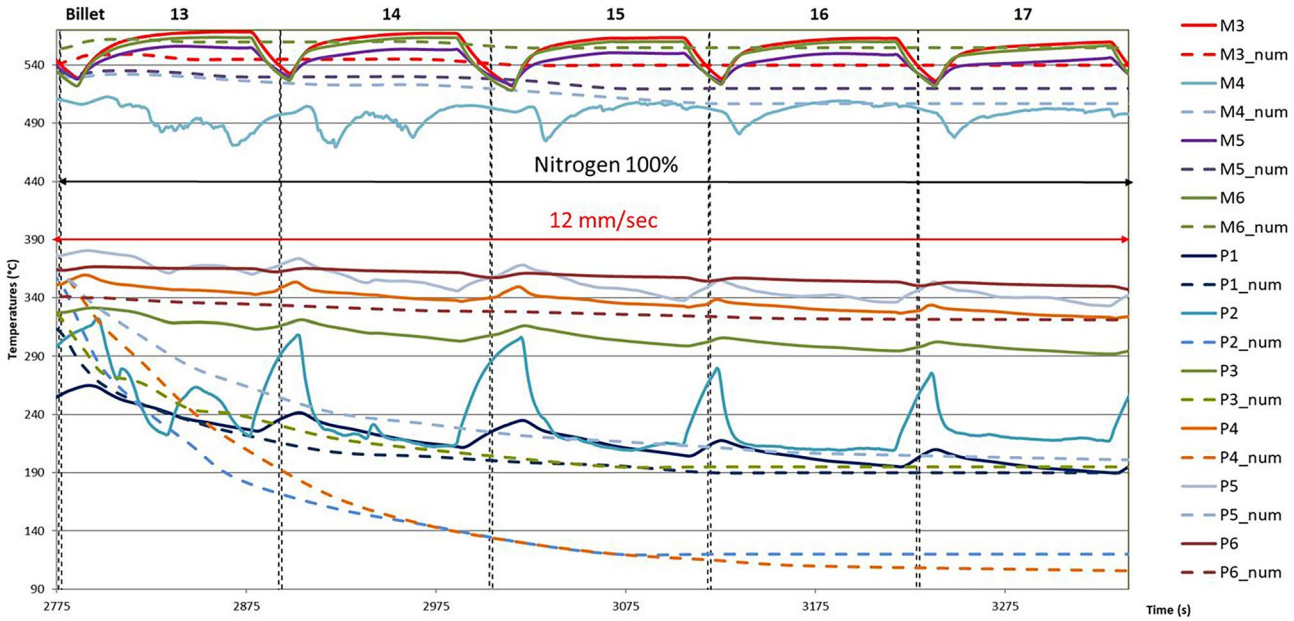

Fig. 13 Temperature history of the extrusion process: Experimental–numerical comparison in the liquid cooled condition

an underestimation in P5 and P6. The different matching is related to the time history of the nitrogen phase evolution. In billet 5, the gaseous nitrogen had an effect on P1 to P3 only, while the other locations behaved like in uncooled conditions. In billet 12, the liquid nitrogen started flowing in P1, thus affecting also P2 at the end of billet 12. The remaining locations were affected by the effect of gaseous-liquid mixture with a drop of temperatures during the extrusion of billet 12. Tables 5 and 6 report the comparison of simulated and experimental temperatures at the middle of billet 12 with errors always below 8%. In terms of extrusion load, a simulated peak value of 21 MN was obtained against 24 MN experimentally acquired (error of 12.5%).

In Fig. 13, the simulation data of the liquid cooled condition (100% valve opening and an extrusion ram speed of 12 mm/s) were compared with the experimental data. Results are plotted for billets 13 to 17.

In the die, the increase of ram speed caused an initial raise of temperature in all thermocouples, as visible during the processing of billet 13. Liquid nitrogen cooling generated a decrease of temperatures in M4 and M5, while a negligible cooling was detected in the other thermocouples, in good agreement with the experimental results.

In the backer, the numerical cooling was more effective than in the experimental trials, with a good temperature matching only for P1 due to the presence of liquid–gas mixture nitrogen within the whole channel (from P2 to P5). Finally, a good correlation was also found for P6 with a negligible temperature decrease both in the numerical and the experimental results.

Tables 7 and 8 report in detail data for billet 17. In the backer, a peak error of −67.8% was found in P4 temperature prediction, but in P1 and in P6, the error was 3.1% and 8.3%, respectively. In the die, errors were always below 5%. In terms of extrusion load, both in the numerical prediction and in the experimental results, the increase of loads remained under 10% (numerically, from 20.5 MN of billet 4 to 22 MN of billet 17, experimentally from 23.3 MN to 25.5 MN).

Finally, even if the numerical model of nitrogen cooling does not consider the phase change, the analysis of the nitrogen temperature can provide information about nitrogen phase. With the assumption that all pressure drops in the channel are negligible, the range of pressure within the channel is about 3–4 bars and, in this condition, the boiling temperature of nitrogen is about –186 °C (Fig. 14) [18]. The

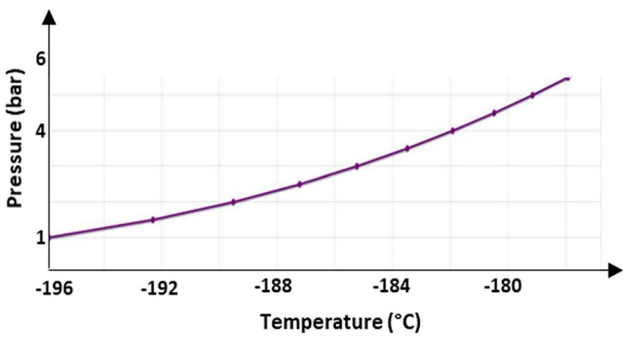

Fig. 14 Boiling point of liquid nitrogen according to the operating pressure

Table 7 Comparison between the experimental acquired temperatures in the backer and the predicted numerical results (Billet 17)

Billet 17	Thermocouples temperature [°C]						Cooling
	P1	P2	P3	P4	P5	P6	
Experimental	196	219	296	326	340	350	**Liquid**
Numerical	190	120	195	105	200	321	**Liquid**
%Err	−3.1%	−45.2%	−34.1%	−67.8%	−41.2%	−8.3%	

Table 8 Comparison between the experimental acquired temperatures in the die and the predicted numerical results (Billet 17)

Billet 17	Thermocouples temperature [°C]					Profile Exit T [°C]	Cooling
	M3	M4	M5	M6	M7		
Experimental	560	502	547	557		541	**Liquid**
Numerical	540	507	520	555	490	555	**Liquid**
%Err	−3.6%	+1.0%	−4.9%	−0.4%		+2.6%	

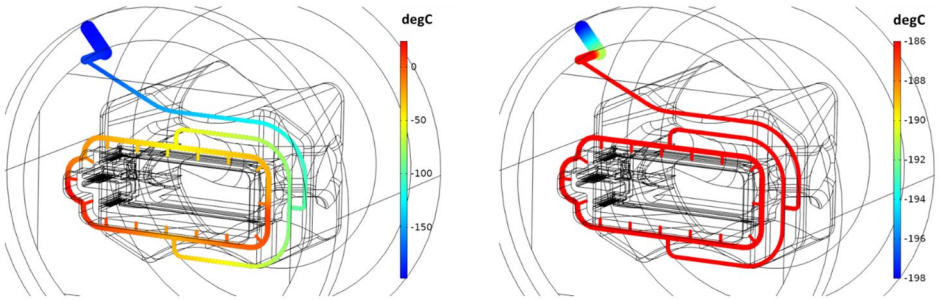

a) **b)**

Fig. 15 Thermal map of liquid nitrogen into the channel (billet 12): **a** range of temperature along the channel, **b** gas formation along the channel

information obtained by the liquid nitrogen thermal map (Figs. 15a, b) of billet 12 confirmed the presence of a big amount of gas along the channel. As can be deduced from Fig. 15a, the temperature is higher than the boiling temperature along the channel, with values of –50 °C nearby P4 and P5 and of about 10 °C nearby P6. Figure 15b shows in red all the points of the cooling path with temperatures higher than the boiling point at 3 bars of pressure. Only nearby the inlet channel, the obtained temperatures suggested the presence of liquid nitrogen as also experimentally evidenced.

The proposed numerical model confirmed a good predictability of the results in terms of thermal field and extrusion load in the uncooled, gaseous cooled and liquid cooled extrusions. Moreover, the analysis clearly highlighted the limits of the tested cooling channel design, emphasising the importance of a proper tool to support the die design.

5 Conclusions

In the present work, an experimental campaign was presented with the aim to investigate the effect of the nitrogen cooling in the extrusion process of aluminium alloys and to validate a multi-physics FE model proposed by the authors that innovatively considered the effect of liquid and gaseous phases of the nitrogen. An industrial porthole die was identified, and the thermal field evolution was strictly monitored by several thermocouples placed nearby the cooling channel and the bearing zones.

The acquired temperatures showed a not optimized channel design that produced an unbalanced cooling in the backer and, to a less extent, in the die. The 40% of nitrogen flow rate was found to be inadequate to promote the liquid nitrogen flow within the channel. The 100% of nitrogen flow rate caused a detectable cooling in the backer only after the extrusion of 4 billets (billet 13) and a similar trend was found, with a minor extent, also in the die. In addition, the experimental results confirmed that a mixture of gas and liquid nitrogen was still present within the channel after a long transitory, and that the steady state cooled condition with liquid nitrogen was not reached experimentally within the 17 extrusions performed, thus limiting the cooling effectiveness.

Concerning the FE model in the previous work by B. Reggiani and L. Donati [24], in which a good matching between numerical and experimental data (peak error of 8%) was found for the liquid nitrogen modelling, there were limitations: on the one hand, the simulation was stationary

and, on the other hand, the 1D model of the cooling channel was used for the simulation of the liquid nitrogen only. In the present work, these limitations were overcome: the transient simulation of the extrusion of multiple billets of an industrial profile using both liquid and gaseous nitrogen modelling was carried out. This study evidenced that the discrete model approach (gaseous cooling only or liquid cooling only) provides clear indication on the average thermal distribution in the backer and in the die however highlighting also possible improvements. Specifically, nitrogen in the channel was experimentally proved to evolve with time from a 100% gaseous state at the beginning of the process to a 100% liquid state when steady-state condition is reached. The developed model was able to get only the two extreme conditions (100% gaseous or 100% liquid) while most of the analysed conditions were in a phase mixture, thus clearly tracing the future developments of the present work.

Even stating the existing limits, the numerical-experimental matching was extremely accurate for the uncooled process as well as for the gaseous and liquid cooling. In more details, the developed model provided estimations with average errors below 5% for the uncooled conditions, below 3% in the die and below 4% in the baker for the gaseous phase while below 3% in the die and 35% in the backer for the liquid phase. These results of the liquid nitrogen predictions overestimate the experimental cooling because the simulation reaches the thermal steady-state faster than what happen in the experiments as the simulation does not consider the mixture of liquid gas nitrogen. In terms of profile temperatures and extrusion loads, errors remained below -1.3% and 12%, respectively, for uncooled simulations, below 0.6% and 13% for gaseous state, and below 2.6% and 14% for liquid state simulations.

The achieved results suggest the reliability of the novel developed simulation tool and its potential integration in a flexible procedure to be used for process and die design optimization. Point of interest for future development is the implementation of new equations in the 1D numerical model in order to include the phase change of nitrogen during the extrusion process.

Author contribution All authors contributed to the study conception and design. Material preparation, data collection and analysis were performed by Riccardo Pelaccia, Barbara Reggiani, Marco Negozio and Lorenzo Donati. The first draft of the manuscript was written by Riccardo Pelaccia and all authors commented on previous versions of the manuscript. All authors read and approved the final manuscript.

Availability of data and materials Not applicable.

Code availability Commercial code COMSOL Multiphysics (software application).

Declarations

Ethics approval and consent to participate Not applicable. Informed consent was obtained from all individual participants included in the study.

Consent for publication The participant has consented to the submission of the case report to the journal.

Competing interests The authors declare no competing interests.

References

1. Saha PK (2000) Aluminum extrusion technology. ASM Int Materials Par, Ohio
2. Sheppard T (1999) Extrusion on Aluminum Alloys. Kluwer Academic Publisher, Boston
3. Staley JT, Liu J, Hunt WH (1997) Aluminum alloys for aerostructures. Adv Mater Process 152(4):17–20
4. Saha PK (1998) Thermodynamics and tribology in aluminum extrusion. Wear 218(2):179–190
5. Parson NC (1996) Surface Defects on 6xxx Alloy Extrusions, vol. 1. In: Proceedings of the 6th International Extrusion Technology Seminar, pp 57–67
6. Qamar SZ, Arif AFM, Sheikh AK (2004) Analysis of product defects in a typical aluminum extrusion facility. Mater Manuf Process 19(3):391–405. https://doi.org/10.1081/AMP-120038650
7. Qamar SZ, Pervez T, Chekotu JC (2018) Die defects and die corrections in metal extrusion. Metals 8(6):380. https://doi.org/10.3390/met8060380
8. Akhtar SS, Arif AFM (2010) Fatigue failure of extrusion dies: effect of process parameters and design features on die life. J Fail Anal Prev 10:38–49. https://doi.org/10.1007/s11668-009-9304-4
9. Stratton P (2008) Raising productivity of aluminium extrusion with nitrogen. Int Heat Treat Surf Eng 2(3–4):105–108. https://doi.org/10.1179/174951508X429221
10. Ward TJ, Kelly RM, Jones GL, Heffron J (1984) Effects of nitrogen - liquid and gaseous - on aluminum extrusion. J Miner Met Mater Soc 36(12):29–33
11. Brodbeck H (1984) Experience Using Liquid Nitrogen for Die Cooling. In: Proceedings of the Third International Aluminum Extrusion Technology Seminar (ET 1984), vol. 1. Atlanta, Georgia, the Aluminum Extruders Council and the Aluminum Association, pp 279–282
12. Marchese MA, Coston JJ (1988) Efficient Use of Liquid Nitrogen for Aluminum Extrusion Die Cooling and Inerting. In: Proceedings of Fourth International Aluminum Extrusion Technology Seminar (ET 1988), vol. 2. Chicago, Illinois, the Aluminum Extruders Council and the Aluminum Association, pp 83–88
13. Mainetti E, Bertoletti M, Wallfish S, Ferrentino A (2012) Significant Extrusion Speed Increase using Liquid Nitrogen to Eliminate Overheating of Dies During Extrusion Process. In: Proceedings of the Tenth International Aluminum Extrusion Technology Seminar (ET 2012), vol. 1. Miami, Florida, Extrusion Technology for Aluminum Profiles Foundation, pp 201–206
14. Donati L, Segatori A, Reggiani B, Tomesani L, Bevilacqua Fazzini PA (2012) Effect of liquid nitrogen die cooling on extrusion process conditions. Key Eng Mater 491:215–222. https://doi.org/10.4028/www.scientific.net/KEM.491.215

15. Reggiani B, Todaro I (2019) Investigation on the design of a novel selective laser melted insert for extrusion dies with conformal cooling channels. Int J Adv Manuf Technol 104(1–4):815–830. https://doi.org/10.1007/s00170-019-03879-9
16. Ronald J, Selines F, Lauricella C (1984) Extrusion Cooling and Inerting Using Liquid Nitrogen. In: Proceedings of the Third International Aluminum Extrusion Technology Seminar (ET 1984), vol. 1. Atlanta, Georgia, the Aluminum Extruders Council and the Aluminum Association, pp 221–226
17. Ciuffini AF et al (2018) Surface quality improvement of AA6060 aluminum extruded components through liquid nitrogen mold cooling. Metals 8(6):409. https://doi.org/10.3390/met8060409
18. Lemmon EW, McLinden MO, Friend DG (2018) Thermophysical Properties of Fluid Systems. In: Linstrom PJ, Mallard WG (eds) NIST Chemistry WebBook NIST Standard Reference Database Number 69. National Institute of Standards and Technology, Gaithersburg
19. Norwood AJ et al (2004) Analysis of cooling channels performance. Int J Comput Integr Manuf 17(8):669–678. https://doi.org/10.1080/0951192042000237528
20. Lurie MV (2008) Modeling of Oil Product and Gas Pipeline Transportation. Wiley-VCH Verlag GmbH & Co KGaA, Weinheim
21. Gnielinski V (1976) New equation for heat and mass transfer in turbulent pipe and channel flow. Int Chem Eng 16:359–368
22. Bastani AF, Aukrust T, Brandal S (2011) Optimisation of flow balance and isothermal extrusion of aluminium using finite-element simulations. J Mater Process Technol 211(4):650–667. https://doi.org/10.1016/j.jmatprotec.2010.11.021
23. Zhang C, Zhao G, Chen H, Guan Y, Kou F (2012) Numerical simulation and metal flow analysis of hot extrusion process for a complex hollow aluminum profile. Int J Adv Manuf Technol 60:101–110. https://doi.org/10.1007/s00170-011-3609-7
24. Reggiani B, Donati L (2019) Prediction of liquid nitrogen die cooling effect on the extrusion process parameters by means of FE simulations and experimental validation. J Manuf Process 41:231–241. https://doi.org/10.1016/j.jmapro.2019.04.002
25. Jiang Y, Wu R, Yuan C, Wang W, Jiao W (2019) Prediction and analysis of breakthrough extruding force based on a modified FE-model in large-scale extrusion process. Int J Adv Manuf Technol 104:3531–3544. https://doi.org/10.1007/s00170-019-04039-9
26. Liu Z, Li L, Yi J, Wang G (2019) Entrance shape design of spread extrusion die for large-scale aluminum panel. Int J Adv Manuf Technol 101:1725–1740. https://doi.org/10.1007/s00170-018-2991-9
27. Reggiani B, Segatori A, Donati L, Tomesani L (2013) Prediction of charge welds in hollow profiles extrusion by FEM simulations and experimental validation. Int J Adv Manuf Technol 69(5–8):1855–1872. https://doi.org/10.1007/s00170-013-5143-2
28. Lou S et al (2017) Analysis and prediction of the billet butt and transverse weld in the continuous extrusion process of a hollow aluminum profile. J Mater Eng Perform 26(8):4121–4130. https://doi.org/10.1007/s11665-017-2771-y
29. Reggiani B, Donati L, Tomesani L (2017) Multi-goal optimization of industrial extrusion dies by means of meta-models. Int J Adv Manuf Technol 88(9–12):3281–3293. https://doi.org/10.1007/s00170-016-9009-2
30. Lou S, Wang Y, Lu S, Su C (2018) Die structure optimization for hollow aluminum profile. Procedia Manuf 15:249–256. https://doi.org/10.1016/j.promfg.2018.07.216
31. Kim YT, Ikeda K (2000) Flow behavior of the billet surface layer in porthole die extrusion of aluminum. Metall Mater Trans A 31:1635–1643. https://doi.org/10.1007/s11661-000-0173-4
32. Qamar SZ (2004) Modeling and Analysis of Extrusion Pressure and Die Life for Complex Aluminum Profiles. King Fahd University of Petroleum & Minerals, Dhahran (Ph.D. Thesis)
33. Sellars CM, McGTegart WJ (1972) Hot workability Int Metall Rev 17(1):1–24
34. Nourani M, Milani AS, Yannacopoulos S (2014) On the effect of different material constitutive equations in modeling friction stir welding: a review and comparative study on aluminum 6061. Int J Adv Eng Technol 7(1):1–20
35. Verlinden B, Suhadi A, Delaey L (1993) A generalized constitutive equation for an AA6060 aluminum alloy. Scr Metall Mater 28:1441–1446. https://doi.org/10.1016/0956-716X(93)90496-F
36. Schikorra M, Donati L, Tomesani L, Tekkaya AE (2007) The Extrusion Benchmark 2007. In: Proceedings of the Extrusion Workshop 2007 and 2nd Extrusion Benchmark Conference, Bologna
37. COMSOL® Multiphysics (Version 5.4). Modelling software. https://www.comsol.it